A protective Langerhans cell-keratinocyte axis that is dysfunctional in photosensitivity

William D. Shipman[1,2,3], **Susan Chyou**[3], **Anusha Ramanathan**[3], **Peter M. Izmirly**[4], **Sneh Sharma**[5,6], **Tania Pannellini**[3], **Dragos C. Dasoveanu**[3,7], **Xiaoping Qing**[3], **Cynthia M. Magro**[8], **Richard D. Granstein**[9], **Michelle A. Lowes**[10], **Eric G. Parmer**[6], **Daniel H. Kaplan**[11,12], **Jane E. Salmon**[2,3,13,14], **Babak J. Mehrara**[15], **James W. Young**[5,6,10,13,16], **Robert M. Clancy**[4], **Carl P. Blobel**[7,13,17,18], and **Theresa T. Lu**[2,3,14,19,*]

[1]Weill Cornell/Rockefeller/Sloan-Kettering Tri-Institutional MD-PhD Program, New York, NY 10065, USA

[2]Immunology and Microbial Pathogenesis Program, Weill Cornell Graduate School of Medical Sciences, New York, NY 10065, USA

[3]Autoimmunity and Inflammation Program, Hospital for Special Surgery, New York, NY 10021, USA

[4]Department of Medicine, New York University School of Medicine, New York, NY 10016, USA

[5]Department of Medicine, Memorial Sloan Kettering Cancer Center, New York, NY 10065, USA

[6]Immunology Program, Sloan Kettering Institute, Memorial Sloan Kettering Cancer Center, New York, NY 10065, USA

[7]Department of Physiology, Biophysics and Systems Biology, Weill Cornell Medicine, New York, NY 10065, USA

[8]Department of Pathology, Weill Cornell Medicine, New York, NY 10065, USA

[9]Department of Dermatology, Weill Cornell Medicine, New York, NY 10065, USA

[10]The Rockefeller University, New York, NY 10065, USA

[11]Department of Dermatology, University of Pittsburgh, PA 15260, USA

[12]Department of Immunology, University of Pittsburgh, PA 15260, USA

[13]Department of Medicine, Weill Cornell Medicine, New York, NY 10065, USA

[14]Rheumatology, Hospital for Special Surgery, New York, NY 10021, USA

*To whom correspondence should be addressed: lut@hss.edu.

[15]Division of Plastic and Reconstructive Surgery, Department of Surgery, Memorial Sloan Kettering Cancer Center, New York, NY 10065, USA

[16]Adult Bone Marrow Transplantation Service, Memorial Sloan Kettering Cancer Center, New York, NY 10065, USA

[17]Arthritis and Tissue Degeneration Program, Hospital for Special Surgery, New York, NY 10021, USA

[18]Institute for Advanced Studies, Technical University Munich, Munich Germany

[19]Department of Microbiology and Immunology, Weill Cornell Medicine, New York, NY 10065, USA

Abstract

Photosensitivity, or skin sensitivity to ultraviolet radiation (UVR), is a feature of lupus erythematosus and other autoimmune and dermatologic conditions, but the mechanistic underpinnings are poorly understood. Here, we identify a Langerhans cell (LC)-keratinocyte axis that limits UVR-induced keratinocyte apoptosis and skin injury via keratinocyte epidermal growth factor receptor (EGFR) stimulation. We show that absence of LCs in Langerin-DTA mice leads to photosensitivity and that, in vitro, mouse and human LCs can directly protect keratinocytes from UVR-induced apoptosis. LCs express EGFR ligands and ADAM17, the metalloprotease that activates EGFR ligands. Deletion of ADAM17 from LCs leads to photosensitivity and UVR induces LC ADAM17 activation and generation of soluble active EGFR ligands, suggesting that LCs protect by providing activated EGFR ligands to keratinocytes. Photosensitive systemic lupus erythematosus (SLE) models and human SLE skin show reduced epidermal EGFR phosphorylation and LC defects, and topical EGFR ligand reduces photosensitivity. Together, our data establish a direct tissue-protective function for LCs, reveal a mechanistic basis for photosensitivity, and suggest EGFR stimulation as a treatment for photosensitivity in lupus erythematosus and potentially other autoimmune and dermatologic conditions.

ONE SENTENCE SUMMARY

Langerhans cells limit ultraviolet radiation-induced keratinocyte apoptosis and skin injury and this axis is dysfunctional in lupus photosensitivity.

INTRODUCTION

Photosensitivity, a sensitivity to ultraviolet radiation (UVR) whereby even ambient sunlight exposure can result in inflammatory skin lesions, is a common feature in cutaneous and systemic forms of lupus erythematosus and can also occur with other autoimmune conditions, a number of dermatologic conditions, and as a response to drugs such as fluoroquinolone antibiotics (1, 2, 3). The photosensitive lesions can be disfiguring and, in systemic lupus erythematosus (SLE), can be associated with systemic disease flares (1, 2). The pathogenesis of photosensitivity is poorly understood and treatments consist mainly of sun avoidance and sunscreen to prevent lesion development (2). A better understanding of the mechanistic basis of photosensitivity could lead to improved disease treatment.

Keratinocyte apoptosis occurs rapidly following UVR exposure, and photosensitivity is associated with increased keratinocyte apoptosis (4, 5). In autoimmune diseases, apoptotic keratinocytes can display autoantigens that bind autoantibodies, leading to complement activation and sustained skin inflammation (1, 5). The localization of "sunburn cells," or apoptotic keratinocytes, with lupus erythematosus skin lesions (6) further supports the idea that keratinocyte apoptosis is part of the pathophysiology. Keratinocytes are critical for normal skin barrier function (7), and, even in the absence of autoimmunity, increased keratinocyte death and failure to compensate has the potential to lead to skin injury and inflammation (8). However, mechanisms that limit UVR-induced keratinocyte apoptosis that are dysfunctional in photosensitivity are not well understood.

In addition to keratinocytes, the epidermis contains a population of well-described Langerin + dendritic antigen-presenting cells, known as Langerhans cells (LCs). LCs are primarily associated with their antigen presentation functions: capturing antigens in the epidermis, migrating from the skin to the draining lymph node, and initiating T cell responses (9, 10). In lupus skin lesions, LCs have an abnormal morphology and are reduced in number (11), suggesting the possibility of a regulatory role. However, in the MRL-Fas^{lpr} SLE mouse model, the role of LCs in spontaneous (i.e. non UVR-induced) skin lesion development has been examined with mixed conclusions; constitutive LC absence had no effect on skin lesions (12) whereas acute depletion of LCs and Langerin+ dermal DCs increased lesions and this was attributed to loss of T cell tolerance (13). Thus, the role of LCs in photosensitivity and as a potential direct modulator of keratinocyte function has not been explored.

We and others have recently shown that dendritic cells (DCs) can directly modulate stromal elements in lymph nodes, adipose tissues, and skin (14-18). As LCs have DC characteristics (9, 10), we asked whether LCs modulated keratinocyte survival and skin injury after UVR exposure. Here we delineate an LC-keratinocyte axis whereby LCs limit UVR-induced keratinocyte apoptosis and skin injury by activating epidermal growth factor receptor (EGFR). This axis is dysfunctional in photosensitive SLE mouse models and there is also evidence of dysfunction in human SLE. Photosensitivity in one of the SLE models is reduced by EGFR ligand supplementation. Together our results identify a tissue protective function for LCs, provide insight into mechanisms that limit skin injury, and suggest that EGFR stimulation may be an approach for treatment of photosensitivity in lupus erythematosus and other diseases.

RESULTS

LCs limit UVR-induced keratinocyte apoptosis and skin injury

LCs are positioned within the epidermis with keratinocytes (Fig. S1A,B), suggesting that LCs have the potential to modulate UVR-induced keratinocyte apoptosis. To test this idea, we used the Langerin-DTA mouse model that is constitutively depleted of LCs (Fig. S1C) but not of Langerin+ dermal DCs (19). We treated wild-type (WT) and Langerin-DTA mice with UVR and examined the skin at 24 hours (Fig. 1A). In WT mice, epidermal LCs were reduced by half with UVR (Fig. S1C), likely due to LC emigration (9, 10) . As expected, UVR induced an increase in activated caspase-3+ cells in the epidermis (Fig. 1B, left).

These cells were Langerin- (Fig. S1D) and CD3- (Fig. S1E), consistent with the idea that the apoptotic cells were keratinocytes. The lack of activated caspase-3+ Langerin+ cells also suggested that LCs were not ingesting apoptotic keratinocytes. Langerin-DTA mice showed increased numbers of activated caspase-3+ keratinocytes relative to WT mice (Fig. 1B, right), and this occurred as early as 3 hours after UVR exposure (Fig. S1F). Langerin-DTA mice had greater monocyte accumulation (Fig. 1C). This was associated with greater numbers of monocyte-derived DCs (Fig. S1G), while CD11b– DCs, CD11 b+ DCs, macrophages, and neutrophils did not increase in Langerin-DTA mice (Fig. S1G). Our UVR source provided both UVA and UVB (20), and increased UVR-induced keratinocyte apoptosis and monocyte accumulation in Langerin-DTA mice remained when UVB was blocked by use of a Mylar filter (Fig. S1H-J), suggesting that LCs limit the effects of at least UVA. Together, these results suggested that LCs limit UVR-induced keratinocyte apoptosis and skin inflammation.

We assessed additional parameters of skin function. UVR exposure induces epidermal hyperplasia within several days (21), and Langerin-DTA mice showed less epidermal thickening than WT mice (Fig. 1D,E). Epidermal barrier function is compromised despite the hyperplasia (22), and Langerin-DTA skin showed greater tissue penetrance of toluidine blue (23) than WT skin (Fig. 1F), suggesting worsened barrier function. Consistent with worsened skin function, Langerin-DTA mice showed a greater lesional area after exposure to multiple UVR doses (Fig. 1G,H, Fig. S1K). These results together suggested that LCs limit the extent of UVR-induced skin injury.

We next attempted to assess whether the monocytes that accumulated in UVR-treated skin contributed to the UVR-induced damage. Consistent with the work of Tamoutounour et al. (24), we identified CCR2+ monocytes and monocyte-derived DCs in inflamed skin, and CD11b+ DCs were also CCR2+ (Fig. S2A). Monocytes and monocyte-derived DCs comprised the vast majority of CCR2+ cells (Fig. S2B). LCs were CCR2– (Fig. S2C). We depleted the CCR2+ cells using CCR2-DTR mice (Fig. S2D)(25). The depletion did not alter UVR-induced keratinocyte apoptosis or epidermal thickness (Fig. S2E,F) but reduced toluidine blue penetrance (Fig. S2G). Although we cannot rule out a role for the CD11b+ DCs, these data raise the possibility that an increased number of infiltrating monocytes and monocyte-derived cells contributed to the worsened barrier function in Langerin-DTA mice.

LCs directly protect keratinocytes

T cells also inhabit the epidermis (9) (Fig. 2A) and we asked whether LCs limited UVR-induced skin injury via T cells. Rag1–/–Langerin-DTA mice lacking both lymphocytes and LCs showed higher UVR-induced keratinocyte apoptosis than Rag1–/– mice (Fig. 2B). While Rag1–/– mice showed higher UVR-induced monocyte accumulation than WT mice (Fig. 2C), Rag1–/–Langerin-DTA mice showed even greater monocyte accumulation (Fig. 2C). These results suggested that LC-mediated skin protection was independent of antigen presentation to T cells and that LCs could potentially limit keratinocyte apoptosis directly.

We tested for direct LC-keratinocyte interactions using LC-keratinocyte cocultures. UVR induces keratinocyte apoptosis in vitro (26), and addition of LCs reduced the apoptosis (Fig. 2D,E). Essentially no activated caspase-3+ cells were Langerin+ (Fig. S3A), suggesting that

the LC-mediated reduction in apoptotic keratinocytes was not due to apoptotic keratinocyte ingestion and clearance. These effects were not due to phototoxicity from the phenol red-containing culture medium as results were similar in phenol red-free medium (Fig. S3B). Together, these results suggested that LCs limit UVR-induced keratinocyte apoptosis and skin injury in vivo by direct interactions with keratinocytes.

LCs limit UVR-induced keratinocyte apoptosis and skin injury by stimulating epidermal EGFR

As keratinocyte EGFR signaling protects against UVR-induced keratinocyte apoptosis (21, 27) and contributes to maintaining epidermal barrier function and limiting skin inflammation (7, 28), we hypothesized that the LC-mediated skin protection involved EGFR signaling. Treatment of WT mice with PD168393, an irreversible EGFR inhibitor (29), reduced epidermal EGFR phosphorylation at tyrosine 1068 (Fig. S4A,B), a residue associated with keratinocyte survival after UVR (27). Ninety-eight percent of epidermal EGFR+ cells were keratinocytes (Fig. S4C,D), suggesting that the epidermal EGFR phosphorylation in Western blots reflected mainly keratinocyte signaling. EGFR inhibition led to increased UVR-induced keratinocyte apoptosis and skin injury (Fig. S4E-H), resembling results from Langerin-DTA mice and supporting the idea that LCs may limit UVR-induced skin injury by modulating keratinocyte EGFR signaling.

We then examined the effects of LC absence on UVR-induced keratinocyte EGFR activation. Epidermal EGFR showed increased phosphorylation by 1 hour after UVR exposure (Fig. S4I) (21), so we assessed this time point in subsequent experiments. The epidermis from Langerin-DTA mice had a modest reduction in homeostatic EGFR phosphorylation (Fig. 3A) and phosphorylation was not upregulated after UVR (Fig. 3B). These results suggested that LCs mediated the UVR-induced keratinocyte EGFR activation.

We asked if the LC-dependent EGFR stimulation was protective for keratinocytes. Treatment of Langerin-DTA mice with HB-EGF, a potent EGFR ligand (30), reduced UVR-induced apoptotic keratinocyte and monocyte accumulation (Fig. 3C,D). In vitro, adding human LCs or HB-EGF to keratinocytes were similar in limiting UVR-induced apoptosis (Fig. 3E, Fig. S5A). Furthermore, siRNA-mediated knockdown of *Egfr* (Fig. S5B) or EGFR inhibition in keratinocytes (Fig. S5C) abolished the protective effect of LCs (Fig. 3F,G) while EGFR inhibition in LCs did not (Fig. S5D,E). Together, these results suggested that LCs limit UVR-induced keratinocyte apoptosis and skin inflammation by stimulating keratinocyte EGFR.

LC ADAM17 is critical for limiting photosensitivity and is activated by UVR

We asked whether LCs could be a key source of EGFR ligands. Both murine and human LCs expressed multiple EGFR ligands, such as epigen and amphiregulin, which were upregulated by UVR exposure in murine LCs (Fig. 4A,B). A disintegrin and metalloprotease 17 (ADAM17) is a membrane-associated metalloprotease that is necessary for the cleavage and activation in cis of all EGFR ligands except EGF and β-cellulin (31), coincidentally, the 2 ligands not expressed or minimally expressed by LCs (Fig. 4A,B). Murine and human LCs expressed ADAM 17 (Fig. S6A-C). The expression of both EGFR ligands and ADAM 17

supported the idea that LCs were potentially capable of directly activating keratinocyte EGFR.

As LCs expressed multiple EGFR ligands, we assessed the role of LC-derived EGFR ligands by crossing ADAM17$^{flox/flox}$ mice (32) with Langerin-Cre$^{+/-}$ mice (33) to generate Langerin-Cre$^{+/-}$ ADAM17$^{flox/flox}$ mice (LC-Ad17 mice) that have *Adam17* constitutively deleted from LCs (Fig. S6D). The Langerin-Cre driver itself had no effect on UVR-induced keratinocyte apoptosis (Fig. S6E), so experiments henceforth used Langerin-Cre $^{-/-}$ADAM17$^{flox/flox}$ mice as controls (WT). Although WT and LC-Ad17 mice had comparable LC numbers (Fig. 4C), LC-Ad17 mice showed reduced UVR-induced EGFR phosphorylation (Fig. 4D), suggesting that LC-derived ADAM17 was important for UVR-induced keratinocyte EGFR activation.

We further asked about the importance of LC ADAM17 in protecting skin. The LC-Ad17 mice showed increased accumulation of apoptotic keratinocytes, monocytes, and monocyte-derived DCs (Fig. 5A,B, Fig. S6F,G), blunted epidermal hyperplasia (Fig. 5C), and increased epidermal permeability (Fig. 5D) after UVR exposure. Inducible deletion in LCs (34) of ADAM17 in Langerin-Cre-ER$^{+/-}$ ADAM17$^{flox/flox}$ mice also increased UVR-induced keratinocyte apoptosis and monocyte accumulation (Fig. S7A-E). HB-EGF treatment dampened the increased UVR-induced keratinocyte apoptosis and skin inflammation in LC-Ad17 mice (Fig. 5E,F), supporting the idea that the effect of LC ADAM17 deletion involved EGFR signals. In vitro, ADAM17-deficiency or blockade rendered LCs unable to protect keratinocytes from UVR-induced apoptosis in both murine and human systems (Fig. 5G,H). These results together strongly supported the idea that LCs limit UVR effects via ADAM17 and stimulating keratinocyte EGFR.

The rapid LC-dependent increase in epidermal EGFR activation with UVR suggested that LC ADAM17 could be activated by UVR. To measure ADAM17 activity, we quantified the level of cell-surface tumor necrosis factor receptor 1 (TNFR1), a substrate for ADAM17 (31). Treatment with PMA, a known ADAM17 activator (31), reduced murine LC TNFR1 in an ADAM17-dependent manner, as expected (Fig. 6A). Similar to PMA, UVR rapidly reduced TNFR1 on both murine and human LCs (Fig. 6A,B). This effect was abrogated by *Adam17* deletion or ADAM17 blockade (Fig. 6A,B). These results suggested that ADAM17 on LCs can be rapidly activated by UVR.

To examine whether the UVR-induced ADAM17 activation actually resulted in EGFR ligand cleavage and release, we collected conditioned supernatants from UVR-exposed LCs and assessed how well the supernatants induced EGFR phosphorylation in EGFR-overexpressing A431 indicator cells (Fig. S8A,B). In contrast to supernatants from murine or human LCs that were not exposed to UVR, supernatants from UVR-exposed LCs induced a robust increase in A431 cell EGFR phosphorylation and *Adam17* deletion or ADAM17 blockade abolished this effect (Fig. 6C,D). UVR has been shown to activate ADAM17 on keratinocytes (35), and UVR exposure also caused murine keratinocytes to release more EGFR ligands, although this effect was less pronounced than that seen in the LCs (Fig. S8C). These data further established that UVR can trigger ADAM17 activation on LCs and showed that this activation can result in greater availability of active EGFR ligand. Together,

our results show a central role for LCs and LC-derived ADAM17 in vivo and UVR-induced ADAM17 activation on LCs ex vivo, suggesting that there is an LC-keratinocyte axis whereby UVR induces LC ADAM17 activation and consequent EGFR ligand cleavage, leading to increased keratinocyte EGFR activation, which limits UVR-induced keratinocyte apoptosis and skin injury.

The LC-keratinocyte axis is dysfunctional in photosensitive SLE models and human SLE

We asked whether photosensitivity in SLE models at least in part reflected dysfunction of this LC-keratinocyte axis. The MRL-*Fas*[lpr] SLE model is a known photosensitive strain, developing more UVR-induced skin pathology than control Balb/c and/or MRL-MpJ mice (36, 37). UVR induces increased apoptotic keratinocyte accumulation in MRL-*Fas*[lpr] mice (Fig. 7A) (36) along with skin plasma cell accumulation (Fig. S9A). Consistent with the possibility of a dysfunctional LC-keratinocyte axis, MRL-*Fas*[lpr] mice showed reduced UVR-induced epidermal EGFR phosphorylation (Fig. 7B).

LC numbers are comparable between MRL-*Fas*[lpr] mice and Balb/c controls (38) and we asked about their ability to protect skin. MRL-*Fas*[lpr] LCs showed a trend toward reduced expression of epigen, the most abundantly expressed EGFR ligand, with UVR, and reduced expression of epiregulin (Fig. S9B), a ligand with relatively low expression (Fig. 4A). *Adam17* mRNA, on the other hand, was reduced in MRL-*Fas*[lpr] mice by about 70% at homeostasis and after UVR exposure (Fig. 7C). Consistent with the reduced *Adam17* expression, MRL-*Fas*[lpr] LCs showed no UVR-induced ADAM17 activation as indicated by TNFR1 changes or release of EGFR ligands (Fig. S9C-D). In vitro, MRL-*Fas*[lpr] LCs did not limit UVR-induced keratinocyte apoptosis (Fig. 7D) while control LCs could limit UVR-induced apoptosis of MRL-*Fas*[lpr] keratinocytes (Fig. 7D), suggesting that LC dysfunction was the critical defect leading to increased UVR sensitivity in MRL-*Fas*[lpr] mice. These data together suggested that MRL-*Fas*[lpr] LCs, because of reduced ADAM17 and potentially because of reduced EGFR ligand expression, were unable stimulate epidermal EGFR, thus contributing to photosensitivity.

We also examined the B6.Sle1yaa model of SLE. These mice carry the Sle1 lupus susceptibility locus derived from lupus-prone NZB2410 mice along with the Y chromosome autoimmune accelerator locus whose activity is attributable to TLR7 duplication (39). The mice develop lymphadenopathy by 3 months (Fig. S10A), splenomegaly and autoantibody production by 4 months, and nephritis by 12 months (40). However, the photosensitivity of this model is unknown. Six week old B6.Sle1yaa mice did not show increased UVR-induced keratinocyte apoptosis (Fig. S10B), but 8-12 month old B6.Sle1yaa mice did (Fig. 7E). Upon multi-day UVR treatment, 8-12 month old B6.Sle1yaa mice developed skin lesions as early as 2 days while B6 mice did not (Fig. S10C). The skin findings were associated with the presence of plasma cells in the skin (Fig. S10D). These results indicated that diseased B6.Sle1yaa mice are photosensitive.

The 8-12 month old B6.Sle1yaa mice also showed reduced UVR-induced epidermal EGFR activation relative to controls (Fig. 7F). LC numbers were unchanged and only the EGFR ligand amphiregulin was reduced (Fig. S10E,F), but B6.Sle1yaa LCs showed reduced *Adam17* mRNA expression (Fig. 7G). These data together suggested that photosensitivity in

both SLE models may be attributable at least in part to a dysfunctional LC-keratinocyte axis whereby LCs are less able to produce activated EGFR ligands to stimulate keratinocyte EGFR.

We examined human SLE skin for signs of a dysfunctional LC-keratinocyte axis. Non-sun-exposed, nonlesional SLE skin showed decreased LC numbers relative to healthy control skin (Fig. 7H), suggesting an abnormality in LC function and a potential for reduced input of EGFR ligands. Epidermal EGFR phosphorylation was also reduced in SLE skin (Fig. 7I). These data support the idea that the LC-keratinocyte axis is dysfunctional in human SLE.

Topical EGFR ligand reduces photosensitivity in an SLE model

We asked whether EGFR ligand supplementation could reduce photosensitivity in MRL-Fas^{lpr} mice. Multi-day UVR exposure has been shown to increase complement and immunoglobulin deposition in skin (36) and we observed that this regimen also led to ulcerations with a neutrophil-dominant infiltrate (Fig. 8A-D, Fig. S11A,B). Topical treatment with HB-EGF (Fig. 8A) reduced the severity of UVR-induced skin lesions (Fig. 8B-D, Fig. S11A,B) and monocyte accumulation (Fig. 8E). Topical HB-EGF also reduced germinal center B cells (Fig. S11C) and plasma cells (Fig. S11D) in skin-draining lymph nodes, suggesting that modulating skin EGFR signaling may impact systemic immunity. These findings suggest that compensating for a dysfunctional LC-keratinocyte axis by providing EGFR ligand can be used as an approach to treating photosensitivity.

DISCUSSION

LCs are best known as antigen-presenting cells, and our findings here establish LCs also as direct modulators of keratinocyte function and skin integrity whereby LCs limit sensitivity to UVR-induced keratinocyte apoptosis and skin injury. The mechanism requires LC expression of ADAM17, the metalloprotease that activates LC-expressed EGFR ligands to stimulate epidermal EGFR. LC abnormalities may contribute to dysfunction of the LC-keratinocyte axis in SLE, leading to photosensitivity, and EGFR ligand supplementation may be an approach to treating photosensitivity (Fig. S12).

The LC-keratinocyte axis appears to be a stress survival mechanism. During homeostasis, keratinocyte ADAM17 plays a major role in maintaining skin integrity and barrier function (23), and our results indicating that LCs have only a modest role in maintaining epidermal EGFR phosphorylation during homeostasis is consistent with this. In contrast, LCs and LC ADAM17 had an important role in limiting skin injury with UVR, suggesting a scenario in which, in times of stress, keratinocytes require an extra source of EGFR ligands and LCs function as this source. That LC ADAM17 responded more robustly to UVR than keratinocyte ADAM17 further supported a role for LCs in providing a critical source of EGFR ligands in the setting of stress. This role in promoting survival during stress is similar to the role of DCs that we have delineated in inflamed lymph nodes and fibrotic skin (14, 15). Murine LCs are closely related to macrophages in ontogeny but have classical DC functions (10). Our findings suggest that LCs behave as DCs in maintaining epidermal integrity in times of stress.

Our model that LCs provide EGFR ligands to stimulate keratinocyte EGFR was supported by the UVR-induced increase in EGFR phosphorylation. In vitro, UVR-induced EGFR phosphorylation has been shown to involve both ligand-induced EGFR kinase activity (35, 41, 42) and reduction of protein receptor type phosphatase kappa activity (43). The inhibition of UVR-induced EGFR phosphorylation by an EGFR tyrosine kinase inhibitor in vivo supports the importance of EGFR kinase activity. Whether LCs also regulate phosphatase activity merits further study.

Our study adds to the recent developments showing rapid EGFR ligand production at barrier surfaces as a protective mechanism. Regulatory T cells and group 2 innate lymphoid cells have recently been shown to be critical sources of the EGFR ligand amphiregulin in protecting lung and colonic epithelium, respectively, during inflammation (44, 45). In these models, amphiregulin expression was induced within days by alarmins from the injured tissues. In contrast, LCs were "immediate responders", as LC-dependent epidermal phosphoEGFR upregulation occurred by 1 hour after UVR in vivo and UVR could act directly on LCs to activate LC ADAM17 ex vivo. Whether injured keratinocyte signals induce the upregulation of LC epigen and amphiregulin at 24 hours and whether LCs are unique among immune cells in direct activation of ADAM17, are unknown. However, our study and others together suggest that there are distinct immediate versus early layers of regulation to protect barrier surfaces.

Hatakeyama et al. (46) recently suggested that LCs help to resolve UVR-induced skin inflammation at day 5 and later after UVR exposure by ingesting and clearing apoptotic keratinocytes. We show distinct findings, focusing on immediate events after UVR exposure. Furthermore, we detected essentially no activated caspase-3+ Langerin+ cells at 24 hours after exposure in WT mice and in LC-keratinocyte co-cultures, suggesting that LC phagocytosis of apoptotic keratinocytes was minimal both in vivo and in vitro. Thus, while we do not rule out a role for LCs in clearing apoptotic keratinocytes at later time points, our study firmly establishes a role for LCs in limiting keratinocyte apoptosis early on.

Our study also suggested that LCs limit monocyte recruitment to the UVR-exposed skin and that accumulated monocytes contribute to increased epidermal permeability. Interestingly, UVR has long been noted to deplete LCs from the skin, and this depletion correlated with myeloid cell accumulation (47). Our results would suggest that the UVR-mediated depletion of LCs caused the myeloid cell accumulation and that stronger or chronic UVR exposure would further deplete LCs, leading to greater myeloid cell accumulation. EGFR activity has been shown to limit keratinocyte CCL2 expression (7), but the extent to which LCs alter chemokine expression by keratinocytes, fibroblasts, or endothelial cells needs to be examined more directly in future studies. Elkon and colleagues (48) recently showed that monocytes may be a major source of type I interferon a few days after UVR exposure, and it would be interesting to understand whether type I interferon increased epidermal permeability. As UVR is also associated with immune suppression in healthy humans but increased autoimmunity in SLE patients (1, 47), it will be interesting to understand whether monocyte and monocyte-derived cells participate in differentially modulating immunity after UVR exposure in healthy and lupus erythematosus patients.

Our study is relevant for understanding photosensitivity in human disease in several ways. First, we showed that the LC-keratinocyte axis is dysfunctional in two SLE models and the reduced EGFR phosphorylation in human SLE skin suggested that this axis may be dysfunctional and contribute to photosensitivity in human SLE. LC numbers were reduced in human SLE skin, and whether the reduced epidermal EGFR phosphorylation reflected the LC reduction, or other defects such as reduced LC ADAM17 or EGFR ligand expression, remains to be determined. While LC-independent keratinocyte-intrinsic dysfunction may also lead to reduced epidermal EGFR phosphorylation and will need to be considered, the reduced LC numbers suggest failure of LC development or survival or perhaps increased migration to draining lymph nodes and suggest that LCs may be dysfunctional in human SLE. Second, our data showed that LCs protected at least UVA-mediated skin injury. As sunlight is comprised primarily of UVA (49), our data are relevant for better understanding the mechanisms that protect against the effects of sunlight exposure in lupus patients. Further understanding of LC function and regulation in SLE will be interesting, as will understanding whether there are similar defects in photosensitivity associated with other disorders (3).

There are a few limitations of this study. Although epidermal EGFR phosphorylation is reduced in human SLE skin, we do not yet know if human SLE LCs are less able to provide activated EGFR ligands or protect keratinocytes from UVR. We also do not yet understand how UVR activated ADAM17 or how LCs are dysregulated in the SLE models.

Our data suggest that topical EGFR stimulation could be a treatment to prevent the development of photosensitive cutaneous lesions in lupus erythematosus. The reduction in lymph node B cell responses with HB-EGF suggests that EGFR stimulation could also improve the systemic aspects of photosensitivity in SLE. While the potential for carcinogenesis should be considered (50), topical EGF is being investigated for rashes associated with the use of EGFR inhibitors to treat lung cancer patients who are most likely immune compromised (51) (clinicaltrials.gov; trials NCT03051880 and NCT03047863). Furthermore, in mouse models of colitis-associated cancer, EGFR inhibited tumor development, likely by improving epidermal function and reducing inflammation (52). Our findings suggest that EGFR-stimulating agents should be investigated for photosensitivity in lupus erythematosus and potentially other autoimmune and dermatologic conditions.

MATERIALS AND METHODS

Study design

Controlled experiments were designed using mouse models, in vitro systems, and human skin. Animals were randomly assigned to experimental groups. Sample sizes were determined based on previously published experiments using similar tissues and assays (14, 15). No data were excluded, each experiment was performed with at least 3 biological replicates, and all data were reliably reproduced. Investigators were not blinded to group allocation during experiments and data acquisition. During data analysis, investigators were not blinded for flow cytometry, Western blot, epidermal permeability, and mRNA experiments but were blinded for histology/immunofluorescence and lesion measurements. Sample numbers and numbers of independent experiments are included in each figure

legend. Each symbol in figures represents 1 mouse, human, or biological replicate. Primary data are included in Table S3.

UVR treatments

In vivo: Four FS40T12 sunlamps that emit UVA and UVB at a 40:60 ratio (20) were used as the UVR source. We determined 1000 J/m^2 UVR to be the minimal dose that caused visible dilation in the ears of C57BL/6J mice at 24 hours and used this dose for all experiments unless otherwise indicated. For multi-dose experiments with Langerin-DTA mice, mice were shaved 24 hours before the first UVR exposure. SLE model mice were shaved 24 hours before the first UVR exposure and then exposed to 500 J/m^2 of UVR for 6 consecutive days for lesion development experiments.

In vitro: Mouse and human primary keratinocytes and LCs were exposed to 500 J/m^2 UVR with the same UVR lamps as above.

Statistical analyses

For analyses of experiments with more than two groups, one-way ANOVA was initially used to examine differences among groups. For data that were normally distributed according to the Shapiro-Wilkes test, the ANOVA was followed by the two-tailed unpaired Student's t-test to assess differences between two particular groups. For data that were not normally distributed, the nondirectional non-parametric Mann-Whiney *U* test was used to determine differences between two groups. For analyses of experiments with only two groups, we determined the distribution with the Shapiro-Wilkes test, then used the appropriate statistical test for comparison. The statistical test and measure of uncertainty used for each figure is included in the figure legend.

Supplementary Material

Refer to Web version on PubMed Central for supplementary material.

ACKNOWLEDGEMENTS:

REFERENCES AND NOTES

1. Kuechle MK, Elkon KB, Shining light on lupus and UV. Arthritis Res Ther, 9, 101 (2007). [PubMed: 17284304]

2. Chong BF, Werth VP, in Dubois' Lupus Erythematosus and Related Syndromes (Eighth *Edition*), Hahn BH, Ed. (W.B. Saunders, Philadelphia, 2013), pp. 319–332.

3. Millard TP, Hawk JLM, Photosensitivity disorders: cause, effect, and management. Am J Clin Dermatol 3, 239–246 (2002). [PubMed: 12010069]

4. Golan TD, Elkon KB, Gharavi AE, Krueger JG, Enhanced membrane binding of autoantibodies to cultured keratinocytes of systemic lupus erythematosus patients after ultraviolet B/ultraviolet A irradiation. J Clin Invest 90, 1067–1076 (1992). [PubMed: 1522215]

5. Kuhn A, Wenzel J, Weyd H, Photosensitivity, Apoptosis, and Cytokines in the Pathogenesis of Lupus Erythematosus: a Critical Review. Clin Rev Allerg Immu, 1–15 (2014).

6. Reefman E, de Jong MC, Kuiper H, Jonkman MF, Limburg PC, Kallenberg CG, Bijl M, Is disturbed clearance of apoptotic keratinocytes responsible for UVB-induced inflammatory skin lesions in systemic lupus erythematosus? Arthritis Res Ther 8, R156 (2006). [PubMed: 17014704]

7. Lichtenberger BM, Gerber PA, Holcmann M, Buhren BA, Amberg N, Smolle V, Schrumpf H, Boelke E, Ansari P, Mackenzie C, Wollenberg A, Kislat A, Fischer JW, Rock K, Harder J, Schroder JM, Homey B, Sibilia M, Epidermal EGFR controls cutaneous host defense and prevents inflammation. Sci Transl Med 5, 199ra111 (2013).

8. Raj D, Brash DE, Grossman D, Keratinocyte apoptosis in epidermal development and disease. J Invest Dermatol 126, 243–257 (2006). [PubMed: 16418733]

9. Kashem SW, Haniffa M, Kaplan DH, Antigen-Presenting Cells in the Skin. Annu Rev Immunol 35, 469–499 (2017). [PubMed: 28226228]

10. Doebel T, Voisin B, Nagao K, Langerhans Cells - The Macrophage in Dendritic Cell Clothing. Trends Immunol, 817–828 (2017). [PubMed: 28720426]

11. Sontheimer RD, Pr B, Epidermal Langerhans cell involvement in cutaneous lupus erythematosus. J Invest Dermatol 79, 237–243 (1982). [PubMed: 6215451]

12. Teichmann LL, Ols ML, Kashgarian M, Reizis B, Kaplan DH, Shlomchik MJ, Dendritic cells in lupus are not required for activation of T and B cells but promote their expansion, resulting in tissue damage. Immunity 33, 967–978 (2010). [PubMed: 21167752]

13. King JK, Philips RL, Eriksson AU, Kim PJ, Haider RC, Lee DJ, Singh RR, Langerhans Cells Maintain Local Tissue Tolerance in a Model of Systemic Autoimmune Disease. J Immunol 195, 464–476 (2015). [PubMed: 26071559]

14. Chia JJ, Zhu T, Chyou S, Dasoveanu DC, Carballo C, Tian S, Magro CM, Rodeo S, Spiera RF, Ruddle NH, McGraw TE, Browning JL, Lafyatis R, Gordon JK, Lu TT, Dendritic cells maintain dermal adipose–derived stromal cells in skin fibrosis. J Clin Invest 126, 4331–4345 (2016). [PubMed: 27721238]

15. Kumar V, Dasoveanu DC, Chyou S, Tzeng T-C, Rozo C, Liang Y, Stohl W, Fu YX, Ruddle NH, Lu TT, A dendritic-cell-stromal axis maintains immune responses in lymph nodes. Immunity 42, 719–730 (2015). [PubMed: 25902483]

16. Ivanov S, Scallan JP, Kim KW, Werth K, Johnson MW, Saunders BT, Wang PL, Kuan EL, Straub AC, Ouhachi M, Weinstein EG, Williams JW, Briseno C, Colonna M, Isakson BE, Gautier EL, Forster R, Davis MJ, Zinselmeyer BH, Randolph GJ, CCR7 and IRF4-dependent dendritic cells regulate lymphatic collecting vessel permeability. J Clin Invest 126, 1581–1591 (2016). [PubMed: 26999610]

17. Astarita JL, Cremasco V, Fu J, Darnell MC, Peck JR, Nieves-Bonilla JM, Song K, Kondo Y, Woodruff MC, Gogineni A, Onder L, Ludewig B, Weimer RM, Carroll MC, Mooney DJ, Xia L, Turley SJ, The CLEC-2-podoplanin axis controls the contractility of fibroblastic reticular cells and lymph node microarchitecture. Nat Immunol 16, 75–84 (2015). [PubMed: 25347465]

18. Acton SE, Farrugia AJ, Astarita JL, Mourao-Sa D, Jenkins RP, Nye E, Hooper S, van Blijswijk J, Rogers NC, Snelgrove KJ, Rosewell I, Moita LF, Stamp G, Turley SJ, Sahai E, Reis e Sousa C, Dendritic cells control fibroblastic reticular network tension and lymph node expansion. Nature 514, 498–502 (2014). [PubMed: 25341788]

19. Kaplan DH, Jenison MC, Saeland S, Shlomchik WD, Shlomchik MJ, Epidermal langerhans cell-deficient mice develop enhanced contact hypersensitivity. Immunity 23, 611–620 (2005). [PubMed: 16356859]

20. Polla L, Margolis R, Goulston C, Parrish JA, Granstein RD, Enhancement of the Elicitation Phase of the Murine Contact Hypersensitivity Response by Prior Exposure to Local Ultraviolet Radiation. J Invest Dermatol 86, 13–17 (1986). [PubMed: 3745931]

21. El-Abaseri TB, Putta S, Hansen LA, Ultraviolet irradiation induces keratinocyte proliferation and epidermal hyperplasia through the activation of the epidermal growth factor receptor. Carcinogenesis 27, 225–231 (2006). [PubMed: 16123117]

22. Haratake A, Uchida Y, Schmuth M, Tanno O, Yasuda R, Epstein JH, Elias PM, Holleran WM, UVB-induced alterations in permeability barrier function: roles for epidermal hyperproliferation and thymocyte-mediated response. J Invest Dermatol 108, 769–775 (1997). [PubMed: 9129231]

23. Franzke CW, Cobzaru C, Triantafyllopoulou A, Loffek S, Horiuchi K, Threadgill DW, Kurz T, van Rooijen N, Bruckner-Tuderman L, Blobel CP, Epidermal ADAM17 maintains the skin barrier by regulating EGFR ligand-dependent terminal keratinocyte differentiation. J Exp Med 209, 1105–1119 (2012). [PubMed: 22565824]

24. Tamoutounour S, Guilliams M, Montanana Sanchis F, Liu H, Terhorst D, Malosse C, Pollet E, Ardouin L, Luche H, Sanchez C, Dalod M, Malissen B, Henri S, Origins and functional specialization of macrophages and of conventional and monocyte-derived dendritic cells in mouse skin. Immunity 39, 925–938 (2013). [PubMed: 24184057]

25. Hohl TM, Rivera A, Lipuma L, Gallegos A, Shi C, Mack M, Pamer EG, Inflammatory monocytes facilitate adaptive CD4 T cell responses during respiratory fungal infection. Cell Host Microbe 6, 470–481 (2009). [PubMed: 19917501]

26. Doerner JL, Wen J, Xia Y, Paz KB, Schairer D, Wu L, Chalmers SA, Izmirly PM, Michaelson JS, Burkly LC, Friedman AJ, Putterman C, TWEAK/Fn14 signaling involvement in the pathogenesis of cutaneous disease in the MRL/lpr model of spontaneous lupus. J Invest Dermatol 135, (2015).

27. Iordanov MS, Choi RJ, Ryabinina OP, Dinh T-H, Bright RK, Magun BE, The UV (Ribotoxic) Stress Response of Human Keratinocytes Involves the Unexpected Uncoupling of the Ras-Extracellular Signal-Regulated Kinase Signaling Cascade from the Activated Epidermal Growth Factor Receptor. Mol Cell Biol 22, 5380–5394 (2002). [PubMed: 12101233]

28. Mascia F, Lam G, Keith C, Garber C, Steinberg SM, Kohn E, Yuspa SH, Genetic ablation of epidermal EGFR reveals the dynamic origin of adverse effects of anti-EGFR therapy. Sci Transl Med 5, 199ra110 (2013).

29. Fry DW, Bridges AJ, Denny WA, Doherty A, Greis KD, Hicks JL, Hook KE, Keller PR, Leopold WR, Loo JA, McNamara DJ, Nelson JM, Sherwood V, Smaill JB, Trumpp-Kallmeyer S, Dobrusin EM, Specific, irreversible inactivation of the epidermal growth factor receptor and erbB2, by a new class of tyrosine kinase inhibitor. Proc Natl Acad Sci 95, 12022–12027 (1998). [PubMed: 9751783]

30. Ronan T, Macdonald-Obermann JL, Huelsmann L, Bessman NJ, Naegle KM, Pike LJ, Different Epidermal Growth Factor Receptor (EGFR) Agonists Produce Unique Signatures for the Recruitment of Downstream Signaling Proteins. J Biol Chem 291, 5528–5540 (2016). [PubMed: 26786109]

31. Scheller J, Chalaris A, Garbers C, Rose-John S, ADAM17: a molecular switch to control inflammation and tissue regeneration. Trends Immunol 32, 380–387 (2011). [PubMed: 21752713]

32. Horiuchi K, Kimura T, Miyamoto T, Takaishi H, Okada Y, T. Y, Blobel CP, Cutting edge: TNF-alpha-converting enzyme (TACE/ADAM17) inactivation in mouse myeloid cells prevents lethality from endotoxin shock. J Immunol 179, 2686–2689 (2007). [PubMed: 17709479]

33. Kaplan DH, Li MO, Jenison MC, Shlomchik WD, Flavell RA, Shlomchik MJ, Autocrine/paracrine TGFβ1 is required for the development of epidermal Langerhans cells. J Exp Med 204, 2545–2552 (2007). [PubMed: 17938236]

34. Bobr A, Igyarto B, Haley KM, Li MO, Flavell RA, Kaplan DH, Autocrine/paracrine TGF-beta1 inhibits Langerhans cell migration. Proc Natl Acad Sci 109, 10492–10497 (2012). [PubMed: 22689996]

35. Singh B, Schneider M, Knyazev P, Ullrich A, UV-induced EGFR signal transactivation is dependent on proligand shedding by activated metalloproteases in skin cancer cell lines. Int J Cancer 124, 531–539 (2009). [PubMed: 19003995]

36. Menke J, Hsu MY, Byrne KT, Lucas JA, Rabacal WA, Croker BP, Zong XH, Stanley ER, Kelley VR, Sunlight Triggers Cutaneous Lupus through a CSF-1-Dependent Mechanism in MRL-Faslpr Mice. J Immunol 181, 7367–7379 (2008). [PubMed: 18981160]

37. Horiguchi Y, Furukawa F, Ohshio G, Horio T, Imamura S, Effects of ultraviolet light irradiation on the skin of MRL/I mice. Arch Dermatol Res 279, 478–483 (1987). [PubMed: 3435176]

38. Eriksson AU, Singh RR, Cutting edge: migration of langerhans dendritic cells is impaired in autoimmune dermatitis. J Immunol 181, 7468–7472 (2008). [PubMed: 19017935]

39. Pisitkun P, Deane JA, Difilippantonio MJ, Tarasenko T, Satterthwaite AB, Bolland S, Autoreactive B cell responses to RNA-related antigens due to TLR7 gene duplication. Science 312, 1669–1672 (2006). [PubMed: 16709748]

40. Morel L, Croker BP, Blenman KR, Mohan C, Huang G, Gilkeson G, Wakeland EK, Genetic reconstitution of systemic lupus erythematosus immunopathology with polycongenic murine strains. Proc Natl Acad Sci 97, 6670–6675 (2000). [PubMed: 10841565]

41. Huang RP, Wu JX, Fan Y, Adamson ED, UV activates growth factor receptors via reactive oxygen intermediates. The Journal of Cell Biology 133, 211–220 (1996). [PubMed: 8601609]

42. Sachsenmaier C, Radler-Pohl A, Zinck R, Nordheim A, Herrlich P, Rahmsdorf HJ, Involvement of growth factor receptors in the mammalian UVC response. Cell 78, 963–972 (1994). [PubMed: 7923365]

43. Xu Y, Shao Y, Voorhees JJ, Fisher GJ, Oxidative Inhibition of Receptor-type Protein-tyrosine Phosphatase κ by Ultraviolet Irradiation Activates Epidermal Growth Factor Receptor in Human Keratinocytes. Journal of Biological Chemistry 281, 27389–27397 (2006). [PubMed: 16849327]

44. Monticelli LA, Osborne LC, Noti M, Tran SV, Zaiss DM, Artis D, IL-33 promotes an innate immune pathway of intestinal tissue protection dependent on amphiregulin-EGFR interactions. Proc Natl Acad Sci U S A 112, 10762–10767 (2015). [PubMed: 26243875]

45. Arpaia N, Green JA, Moltedo B, Arvey A, Hemmers S, Yuan S, Treuting PM, Rudensky AY, A Distinct Function of Regulatory T Cells in Tissue Protection. Cell162, 1078–1089 (2015). [PubMed: 26317471]

46. Hatakeyama M, Fukunaga A, Washio K, Taguchi K, Oda Y, Ogura K, Nishigori C, Anti-Inflammatory Role of Langerhans Cells and Apoptotic Keratinocytes in Ultraviolet-B-Induced Cutaneous Inflammation. J Immunol, 2937–2947 (2017). [PubMed: 28893957]

47. Cooper KD, Oberhelman L, Hamilton TA, Baadsgaard O, Terhune M, LeVee G, Anderson T, Koren H, UV exposure reduces immunization rates and promotes tolerance to epicutaneous antigens in humans: relationship to dose, CD1a-DR+ epidermal macrophage induction, and Langerhans cell depletion. Proc Natl Acad Sci 89, 8497–8501 (1992). [PubMed: 1382291]

48. Sontheimer C, Liggitt D, Elkon KB, Ultraviolet B Irradiation Causes Stimulator of Interferon Genes–Dependent Production of Protective Type I Interferon in Mouse Skin by Recruited Inflammatory Monocytes. Arthritis Rheumatol 69, 826–836 (2017).

49. Kollias N, Ruvolo E, Jr., Sayre RM, The value of the ratio of UVA to UVB in sunlight. Photochem Photobiol 87, 1474–1475 (2011). [PubMed: 21770951]

50. Uribe P, Gonzalez S, Epidermal growth factor receptor (EGFR) and squamous cell carcinoma of the skin: molecular bases for EGFR-targeted therapy. Pathology, research and practice 207, 337–342 (2011).

51. Shin JU, Park JH, Cho BC, Lee JH, Treatment of epidermal growth factor receptor inhibitor-induced acneiform eruption with topical recombinant human epidermal growth factor. Dermatology 225, 135–140 (2012). [PubMed: 23006507]

52. Dubé PE, Yan F, Punit S, Girish N, McElroy SJ, Washington MK, Polk DB, Epidermal growth factor receptor inhibits colitis-associated cancer in mice. J Clin Invest 122, 2780–2792 (2012). [PubMed: 22772467]

53. Izmirly PM, Shvartsbeyn M, Meehan S, Franks A, Braun A, Ginzler E, Xu SX, Yee H, Rivera T, Esmon C, Barisoni L, Merrill JT, Buyon JP, Clancy RM, Dysregulation of the Microvasculature in Nonlesional Non-Sun-exposed Skin of Patients with Lupus Nephritis. J Rheumatol 39, 510–515 (2012). [PubMed: 22298906]
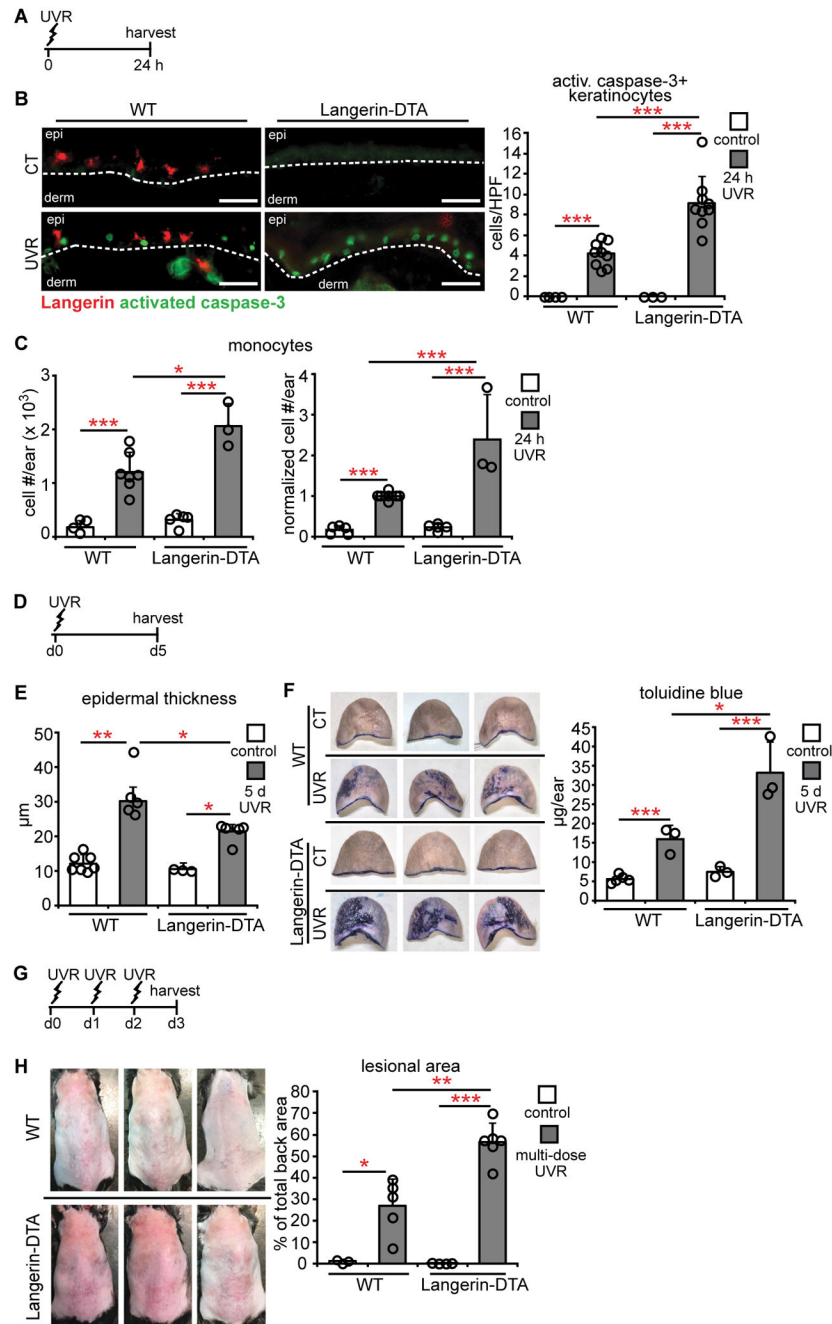
Fig. 1. LCs limit UVR-induced keratinocyte apoptosis and skin injury.

(A-H) WT and Langerin-DTA mice were exposed to UVR and examined. **(A)** Experimental scheme for **(B,C)**; ears were harvested 24 hours after UVR. **(B)** Activated caspase-3+ keratinocytes per high powered field (HPF). Left: Representative images of Langerin (red) and activated caspase-3 (green) stain. Right: Quantification (n= 3-9 mice). Scale bars: 50 μm. **(C)** Absolute (left) and normalized (right) monocyte numbers assessed by flow cytometry (n= 3-7). **(D)** Experimental scheme for **(E,F)**; ears were harvested 5 days after UVR. **(E)** Epidermal thickness (n= 3-7 mice). **(F)** Epidermal permeability as assessed by toluidine blue penetrance. Left: Representative images. Right: Quantification (n= 3-5 mice).

(G) Experimental scheme for **(H)**; mice were exposed to UVR for 3 days and examined 24 hours later. **(H)** Left: Representative images of back skin. Right: Lesional area quantification (n= 3-5 mice). Bars represent means. **(B,C,F,H)** or medians **(E)**. Error bars depict standard deviations **(B,C,F,H)** or interquartile ranges **(E)**. *p<0.05, **p<0.01, ***p<0.001 using two-tailed unpaired Student's t-test **(B,C,F,H)** or nonparametric non-directional Mann-Whitney *U* test **(E)** after one-way analysis of variance (ANOVA). Data are from 9 **(B)**, 5 **(C)**, 4 **(E)**, 2 **(F)**, and 3 **(H)** independent experiments.
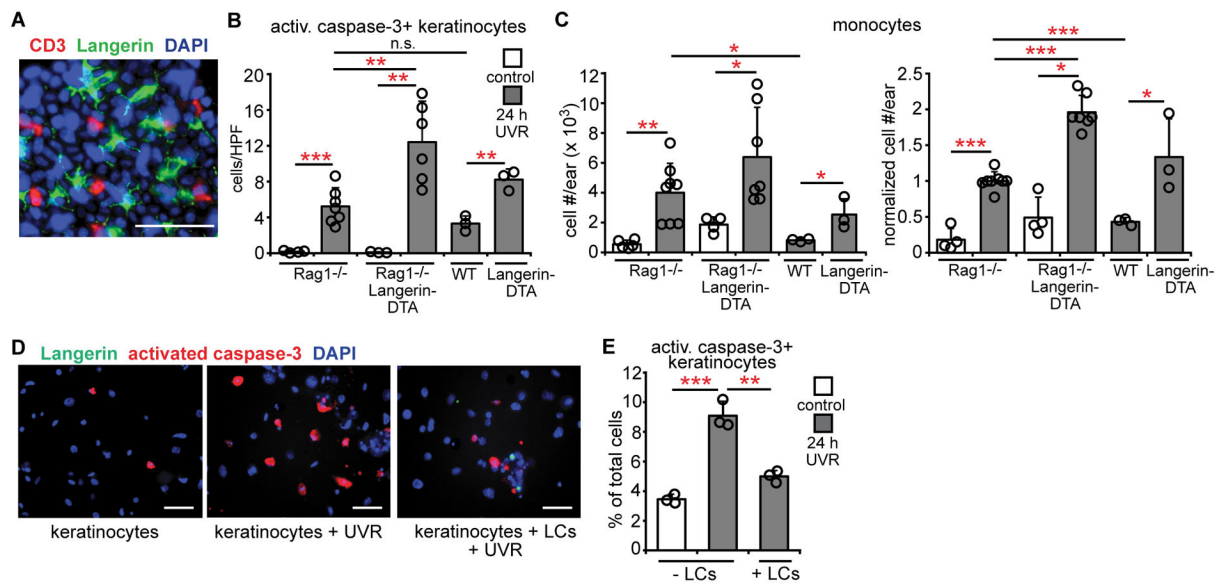
Fig. 2. LCs limit UVR-induced keratinocyte apoptosis directly.
(A) Whole mount stain of homeostatic mouse epidermis for CD3 (red), Langerin (green), and DAPI (blue). **(B,C)** Rag1−/−, Rag1−/−–Langerin-DTA, WT, and Langerin-DTA mice were exposed to UVR and ears were harvested 24 hours later (n= 3-8 mice). **(B)** Activated caspase-3+ keratinocytes. **(C)** Absolute (left) and normalized (right) monocyte numbers. **(D,E)** Effect of LCs on keratinocyte survival in vitro. Murine keratinocyte cultures without and with LCs were exposed to UVR and examined 24 hours later (n= 3 mice). **(D)** Representative images of cultures stained for Langerin (green), activated caspase-3 (red), and DAPI (blue). **(E)** Activated caspase-3+ keratinocytes. **(E)** Data are from 5 **(B,C)** and 3 **(A,D,E)** independent experiments. Scale bars: 50 μm. **(B,C,E)** Bars represent means. Error bars depict standard deviations. *p<0.05, **p<0.01, ***p<0.001 using two-tailed unpaired Student's t-test after one-way ANOVA.
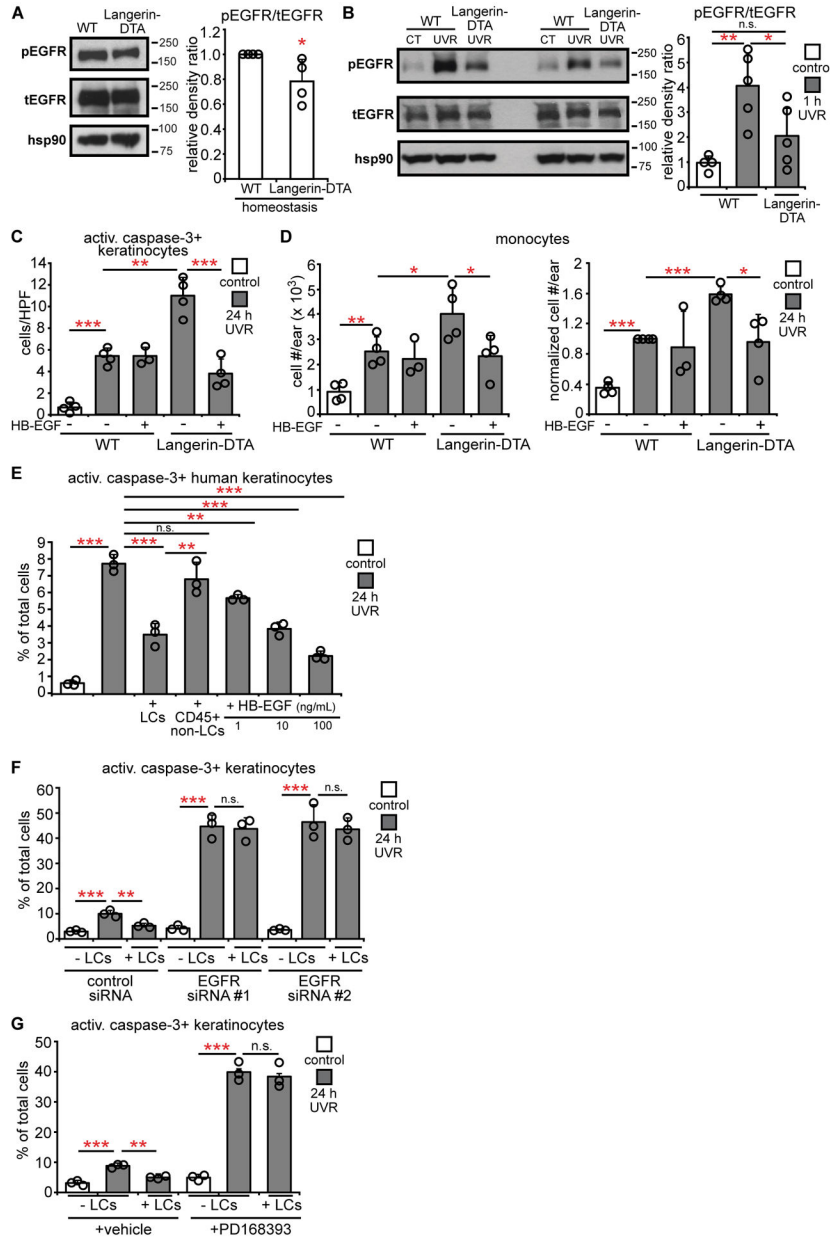
Fig. 3. LCs are required for UVR-induced epidermal EGFR activation and protect keratinocytes via EGFR stimulation.

(A,B) Epidermal EGFR phosphorylation at homeostasis **(A)** and 1 hour after UVR **(B)** (n= 4-5 mice). Left: Representative Western blot for phosphoEGFR (pEGFR), total EGFR (tEGFR), and hsp90 (loading control). Right: pEGFR:tEGFR relative density ratio. Uncropped blots in Fig. S13. **(C,D)** Mouse ears were treated with vehicle or HB-EGF prior to UVR and examined 24 hours after UVR (n= 3-4 mice). **(C)** Activated caspase-3+ keratinocytes. **(D)** Absolute (left) and normalized (right) monocyte numbers. **(E)** Effect of human LCs on UVR-induced keratinocyte apoptosis. Primary human keratinocytes without or with indicated cells or recombinant HB-EGF were exposed to UVR and examined 24 hours later (n= 3 human donors). **(F,G)** Effect of keratinocyte EGFR knockdown and

inhibition on LC-mediated protection. Primary murine keratinocytes were treated with EGFR-targeted or control siRNAs **(F)** or PD168393 **(G)** before LC co-culture and UVR exposure (n= 3 mice). Bars represent means. Error bars depict standard deviations. Data are from 2 **(A,B,F,G),** 4 **(C,D)**, and 3 **(E)** independent experiments. *p< 0.05, **p< 0.01, ***p< 0.001 using two-tailed unpaired Student's t-test. T-test was performed after one-way ANOVA for **(B-G)**.
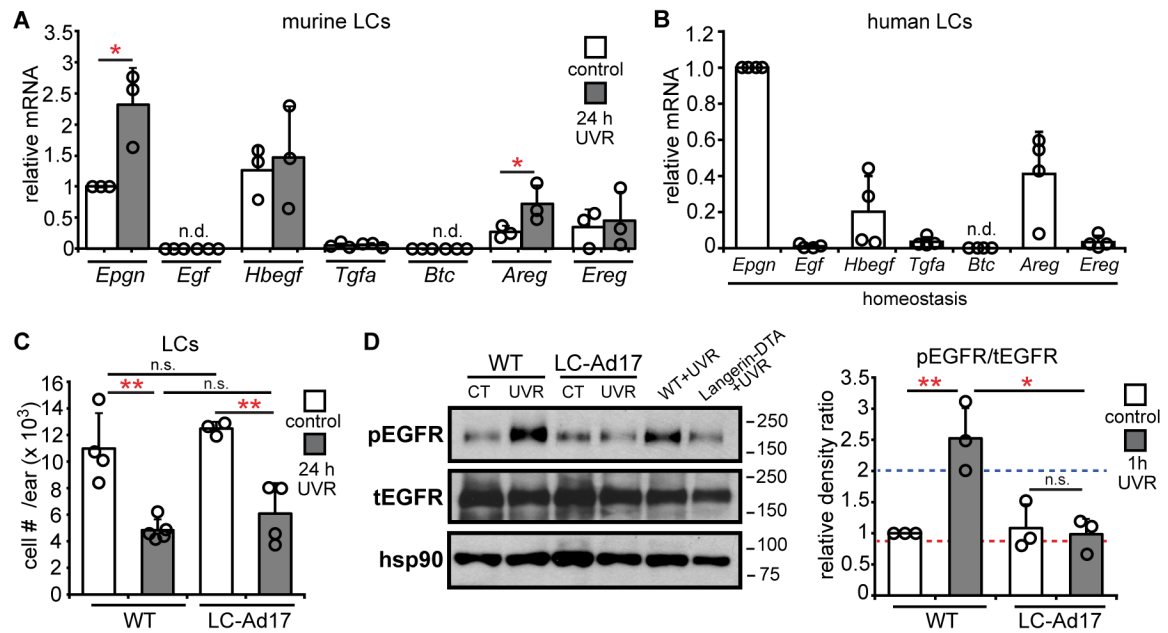
Fig. 4. LCs express EGFR ligands and LC-derived ADAM 17 mediates UVR-induced epidermal EGFR phosphorylation.
(A,B) Murine (A) and human (B) LC EGFR ligand expression (n=3-4 mice or human donors). Murine LCs were sorted from control or UVR-exposed mice. Expression of each ligand was normalized to control murine *Epgn* or human *Epgn* expression. **(C,D)** WT and LC-Ad17 mice were treated with UVR and analyzed at indicated time points. **(C)** LC numbers (n= 3-5 mice). **(D)** Epidermal EGFR phosphorylation. Left: Representative Western blot. Right: pEGFR:tEGFR ratio. Dashed lines are the values for the UVR-exposed WT (blue) and Langerin-DTA (red) mice shown in the blot. Uncropped blots in Fig. S13. Data are from 3 **(A,B)**, 4 **(C)**, and 2 **(D)** independent experiments. Bars represent means. Error bars depict standard deviations. n.s.= not significant p 0.05, *p<0.05, **p<0.01 using two-tailed unpaired Student's t-test. T-test was performed after one-way ANOVA for **(C,D)**.
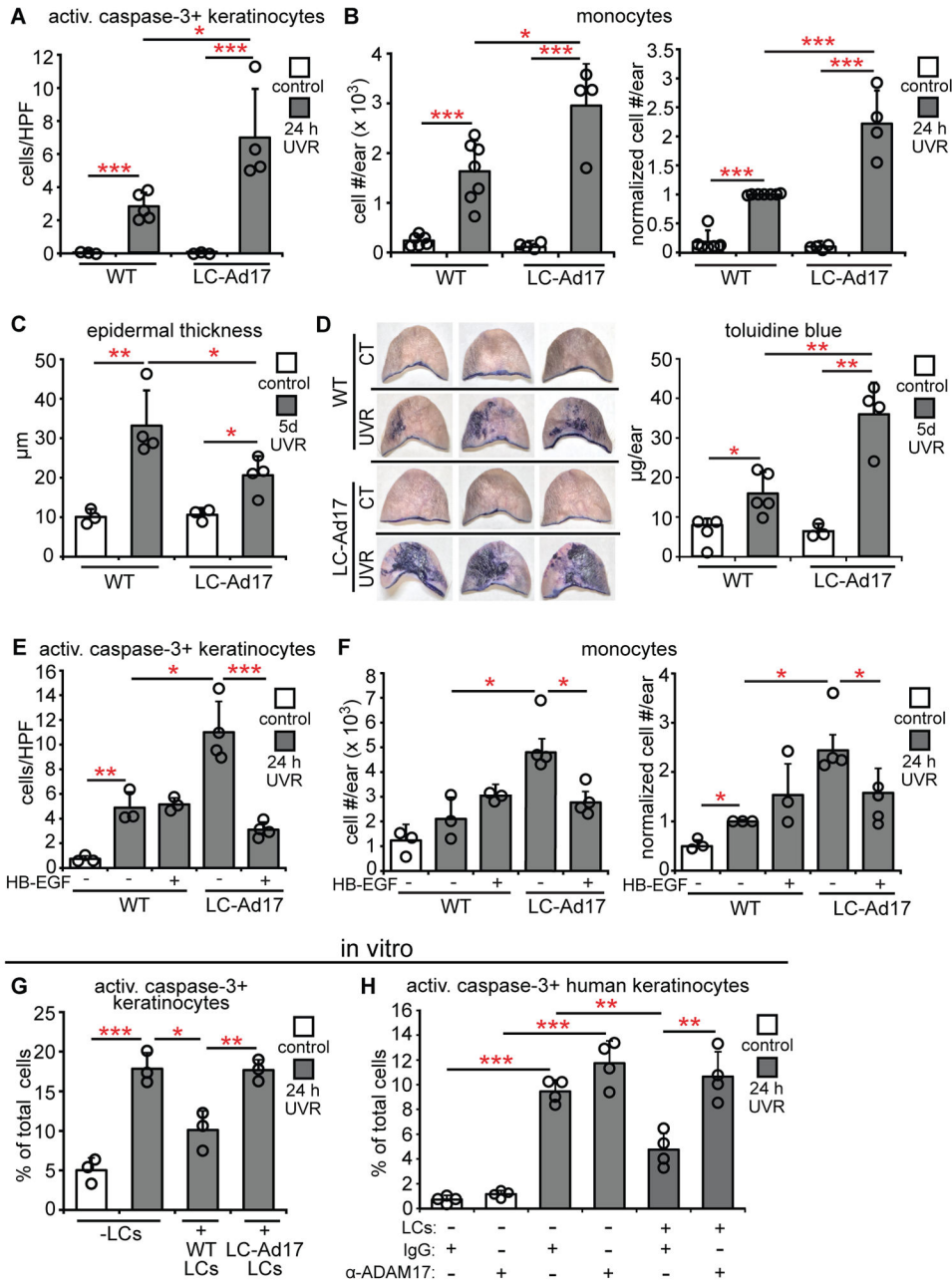
Fig. 5. LC-derived ADAM 17 limits UVR-induced keratinocyte apoptosis and skin injury.
(**A-D**) WT and LC-Ad17 mice were treated with UVR and analyzed at indicated time points.
(**A**) Activated caspase-3+ keratinocytes (n= 3-5 mice). (**B**) Absolute (left) and normalized
(right) monocyte numbers (n= 4-7 mice). (**C**) Epidermal thickness (n= 3-mice). (**D**)
Epidermal permeability (n= 3-5 mice). Left: Representative images. Right: Quantification.
(**E,F**) Vehicle or HB-EGF was applied on the ears prior to UVR exposure (n= 3-4 mice). (**E**)
Activated caspase-3+ keratinocytes. (**F**) Absolute (left) and normalized (right) monocyte
numbers. (**G,H**) Effect of LC *Adam17* deletion or ADAM17 blockade on keratinocyte
survival in vitro. Murine keratinocytes with LCs from indicated mice (**G**) and human
keratinocytes with control-IgG or anti-ADAM17-treated LCs (**H**) were exposed to UVR and

examined at 24 hours (n= 3 mice or 4 human donors). Data are from 3 **(E-G),** 4 **(A)**, 2 **(H)**, 5 **(B)**, and 1 **(C,D)** independent experiments. Bars represent means **(A,B,D-H)** or medians **(C)**. Error bars depict standard deviations **(A,B,D-H)** or interquartile ranges **(C)**. n.s.= not significant p 0.05, *p<0.05, **p<0.01, ***p<0.001 using two-tailed unpaired Student's t-test **(A,B,D-H)** or nonparametric non-directional Mann-Whitney *U* test **(C)** after one-way ANOVA.
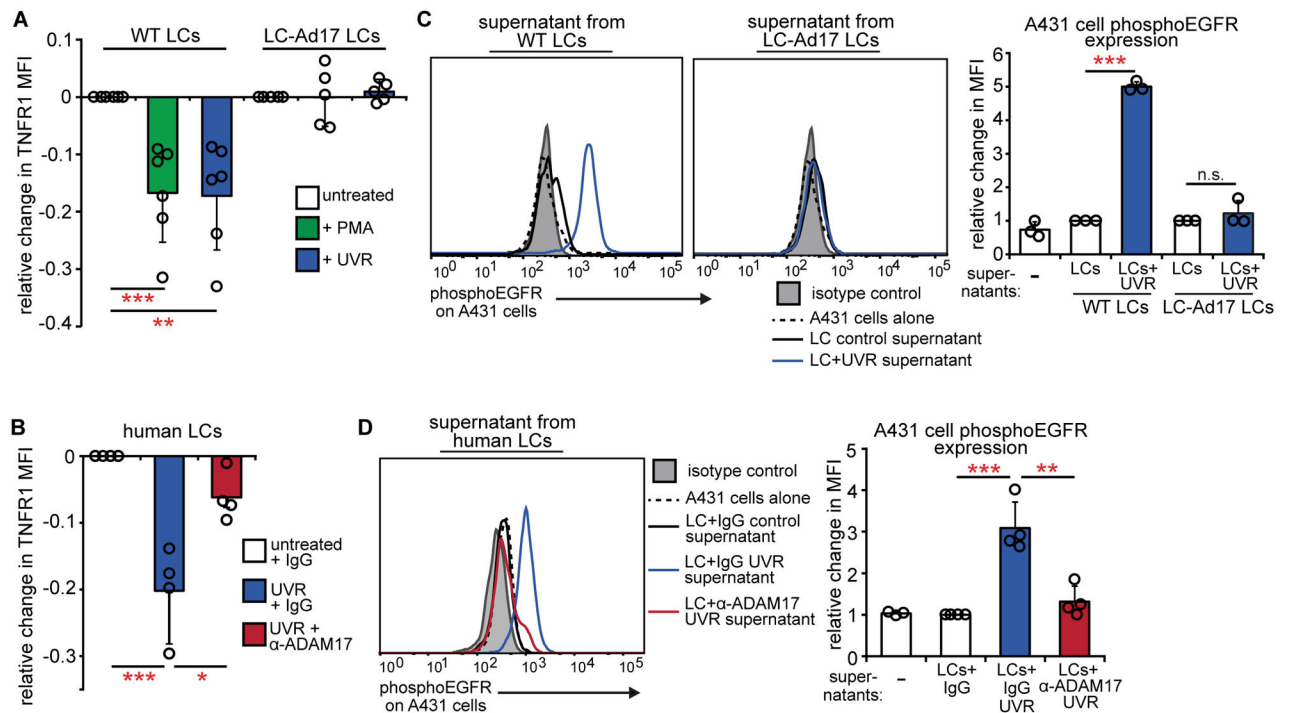
Fig. 6. UVR directly activates LC ADAM17 and EGFR ligand release.
(**A, B**) Effect of UVR on ADAM17 activity in sorted murine (**A**) and human (**B**) LCs as measured by change in TNFR1 mean fluorescence intensity (MFI) 45 minutes after the indicated treatments. PMA is a positive control. (n= 5-6 mice; n=4 human donors). (**C,D**) Conditioned supernatants from murine (**C**) or human LCs (**D**) were added to A431 EGFR indicator cells and phosphoEGFR was measured 10 minutes later by flow cytometry. Murine LC supernatants were from (A); human LC supernatants were from cells treated similarly to (B), except that antibody was washed out prior to UVR (see Supplementary Methods). Left: Representative histogram. Right: Quantification relative to cells treated with control WT LC supernatants (**C**) or control IgG-treated LC supernatants (**D**). Results are from 6 (**A**), 2 (**B,D**), and 3 (**C**) independent experiments. Bars represent means. Error bars depict standard deviations. n.s.= not significant p 0.05, *p<0.05, **p<0.01, ***p<0.001 using two-tailed unpaired Student's t-test after one-way ANOVA.
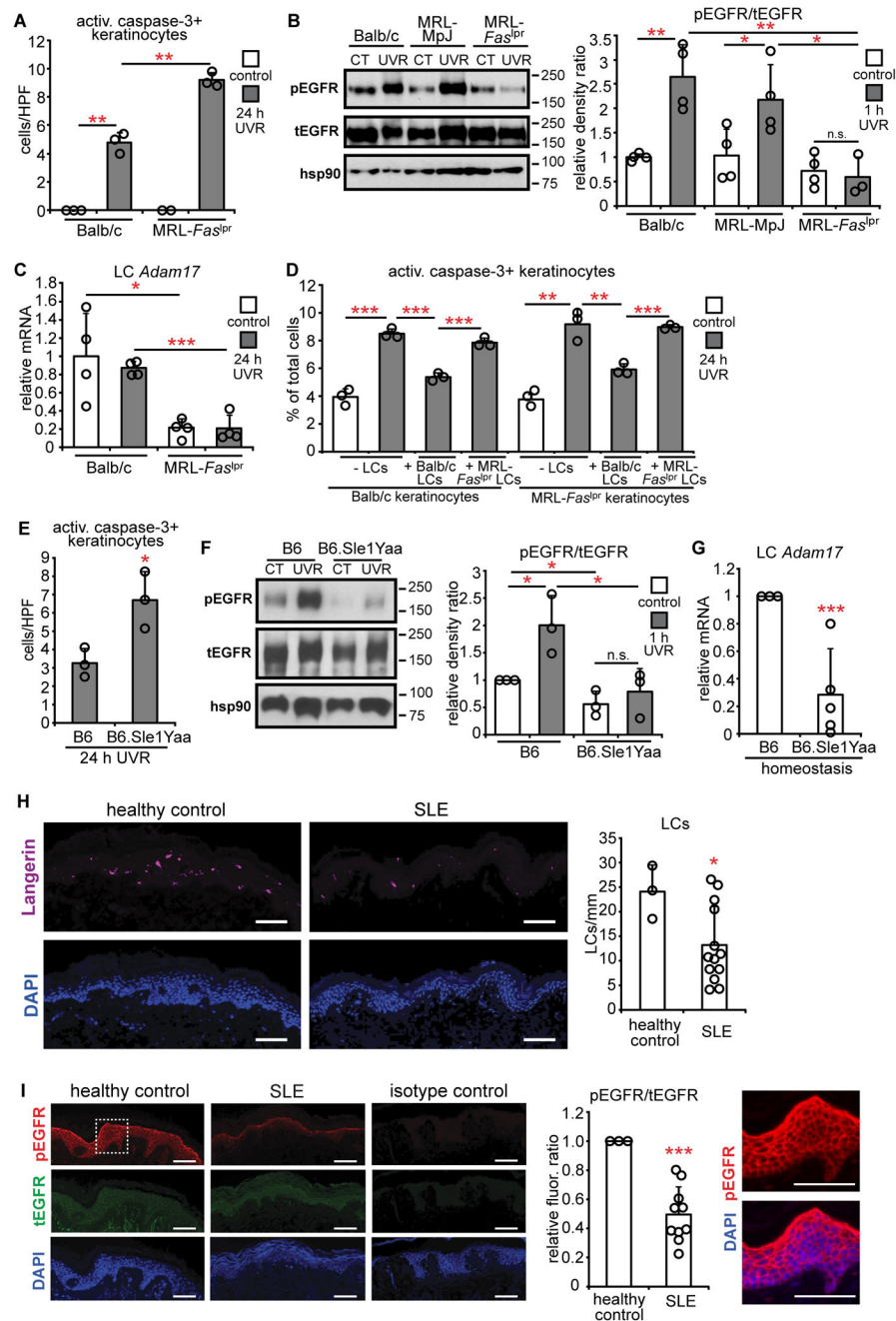
Fig. 7. Photosensitive SLE mouse models and human SLE skin show a dysfunctional LC-keratinocyte axis.
WT and MRL-*Fas*^lpr(n= 2-4 mice) **(A-C)** or B6.Sle1Yaa mice (n= 3-5 mice) **(E-G)** were treated and examined as indicated. **(A,E)** Activated caspase-3+ keratinocytes. **(B,F)** Epidermal EGFR phosphorylation 1 hour after UVR. Left: Representative Western blot. Right: pEGFR:tEGFR ratio. Uncropped Western blots in Fig. S13. **(C,G)** LC *Adam17* expression. **(D)** Effect of MRL-*Fas*^lpr LCs on keratinocyte apoptosis. Balb/c or MRL-*Fas*^lpr keratinocytes were exposed to UVR without or with indicated LCs. (n= 3 mice). **(H,I)** LC numbers and epidermal EGFR phosphorylation in human SLE skin (n= 3 healthy controls,

10-13 SLE patients). **(H)** Left: Representative images of anti-Langerin (purple) and DAPI (blue) staining. Right: LC numbers per mm of tissue. **(I)** Left: Representative images of anti-pEGFR (red), anti-tEGFR (green), and DAPI (blue) staining. Middle: Relative pEGFR:tEGFR fluorescence intensity normalized to healthy control skin. Right: Magnified inset from pEGFR and DAPI stain. Data are from 3 **(A,B,D,E,G-I),** and 2 **(C,F)** independent experiments. Bars represent means. Error bars depict standard deviations. n.s= not significant p 0.05, *p<0.05, **p<0.01, ***p<0.001 using two-tailed unpaired Student's t-test. T-test was performed after one-way ANOVA for **(A-D, F)**.
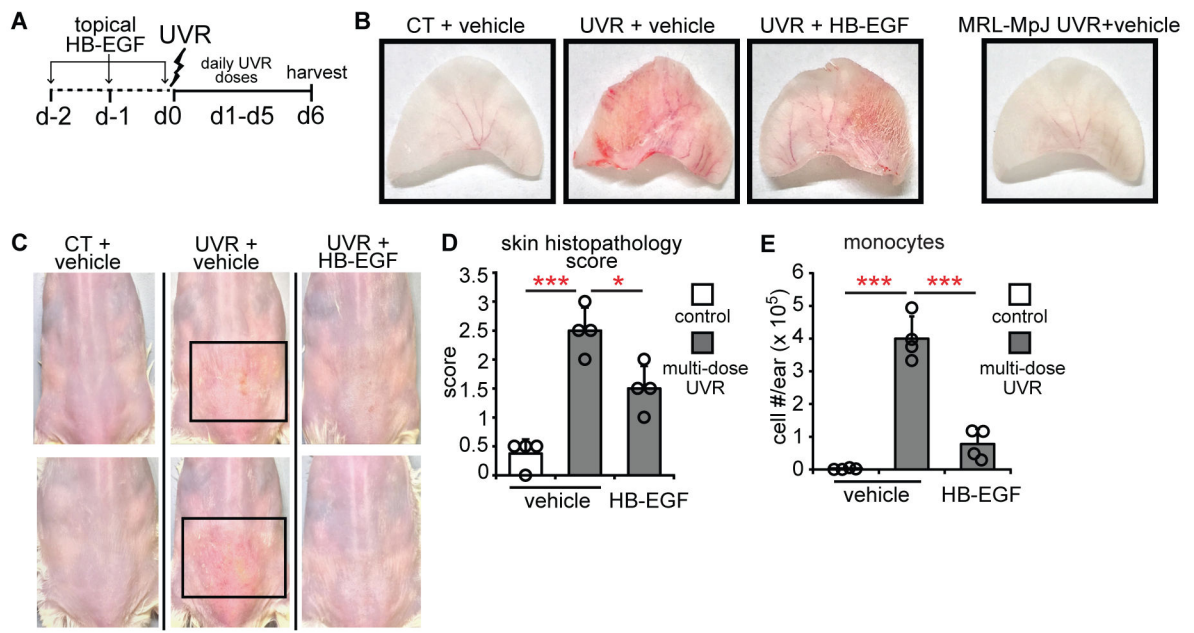
Fig. 8. Topical EGFR ligand reduces photosensitivity.
(**A**) Experimental scheme for (**B-E**) (n= 4 mice). MRL-*Fas*[lpr] mice ears and back skin were topically treated with HB-EGF for 2 days before and on the first day of UVR exposure and examined 24 hours after the final exposure. (**B**) Representative images of ears. The MRL-MpJ ear represents a non-SLE control. (**C**) Representative images of back skin; boxes outline lesional areas. Magnified images of back skin in Fig. S11. (**D**) Ear histopathology score. (**E**) Absolute monocyte numbers. (**B-E**) Data are from 3 independent experiments. Bars represent means. Error bars depict standard deviations. *p<0.05, ***p<0.001 using two-tailed unpaired Student's t-test after one-way ANOVA.